American Journal of Botany and Bioengineering
https://biojournals.us/index.php/AJBP
ISSN: 2997-9331

Plasmonic Nanoparticles for Large-Area, High-Enhancement Surface-Enhanced Raman Scattering Sensors

Ahmed Ayad Madhloom
University of Technology Department of Applied Sciences, Branch Laser science and technology

Hussein Abbas Ali
Technological University, Department of Applied Sciences, Laser Science and Technology

Received: 2024 19, Nov
Accepted: 2024 28, Nov
Published: 2024 09, Dec

Annotation: Silicon technology offers almost unlimited possibilities and pervades our day life the main reason in the information technology is to have the possibility of integrating low – dimensional structures showing appropriate optoelectronic properties with well-established and highly advanced silicon microelectronics technology.

The structural and morphological properties of electrochemically etched porous silicon are investigated using SEM, The porous silicon layers were formed in 40% HF solution and ethanol of 99% in a ratio of n-type silicon. The surface morphology as characterized by scanning electron microscope reveals that the variation in etching time can produce microscopic roughness on the etched surfaces.

The AuNPAs/PS that deposited on porous silicon nano-photonic sensors have been used for performing SERS detections of low concentration of chlorpyrifos pesticide, with concentration 25*10-8 to 3*10-5 M.

1.1. Introduction

The pesticides detection level in the environment is of great importance to regulate and monitor its uses. The interest to study pesticides was triggered since early 1970s. It started by immunoassay-based test and solid phase technology [1]. In order to detect pesticides, numerous analytical methods, including gas chromatography-mass spectrum, liquid chromatography mass spectrometry, and enzyme-linked immunity saturation adsorption. Although these analytical methods have been successful in many reports, there are still limitations from poor detection limit, indirect measurements, and time consuming process. Above that, they have limited the action field besides the inaccurate results obtained. This has triggered the researchers to look for a reliable, portable and accurate way for determining the presence of pesticides [2].

pesticides are substances used to kill, control or repel plants or animals that are considered as pest by physically, chemically or biologically interfere with their metabolism or behavior. Pesticides include herbicide, insecticides, fungicides and disinfectants [3,4]. The last years, there has been an extensive use of agriculture chemicals in food production, making the people exposed to significant pesticides residues through the food [5].

The metallic porous Si shows unique advantage for active SERS substrate, due to large active surface area, high absorption ability and high reproducibility [6,7].

The most significant aspect of silicon nanocrystallite layer is the ability to charge the morphological characteristics of its surface, which means an effective control on the plasmatic metallic nanoparticles via immersion plating represents as an efficient, low cost, simple and effective approach for fabrication SERS sensors.

This method does not require vacuum, a source of energy or any reducing agents. The production of reproducible, inexpensive substrates is an aspect of SERS that has gained much attention [8].

1.2. Historical review

In 2015 Zhai C et al. [9], used AuNPs enhance Raman signal and detect chlorpyrifos in apples by using SERS. This work showed a linear relation between the concentration of chlorpyrifos and the spectral intensity of the SERS characteristic peaks with a detection limit of 0.13 mg/kg.

In 2018 Xuexian C et al [10] synthesized silicon nanowire by metal assisted chemical etching. A detection limit of less than 10-6 M of methylene blue was achieved. This was further improved to about 10-8 M after functionalizing the silicon substrates by using plasmatic AuNPs.

In 2019, yong He et al [11] synthesized ultrasensitive gold nanoparticles of variable particle sizes as SERS substrates to detect CPF in soil. The limit of detection LOD they obtained was 10 microg/L.

In 2020, Bingxue Hu et al [12]. Firstly, a large area high density Au NRs array was fabricated by organic-aqueous interfacial self- assembly to serve as a sensitive SERS substrate for simultaneously screening of thiram and thiabendazole on the fruit surface. The limits of detection (LOD) of pesticides on the surface of apple, tomato and pear were 0.041, 0.029 and 0.047 ng/cm2 for thiram, and 0.79, 0.76 and 0.80 ng/cm2 for thiabendazole, respectively.

1.3. Aim of the project

1. Produce porous silicon layer by photochemical etching process .
2. Study the effect of etching time on porous silicon structure
3. Study the morphological and structural properties of etched layer.
4. In addition, develop an efficient chemical sensor for low pesticides concentration for cholrpyrifos pesticide.

5. This goal was satisfied by fabricating AuNPs /PSi structure chemical SERS sensors.

Crystalline silicon (C-Si) is one of the most important materials of the last century that has been the cornerstone of the semiconductor industry and has extraordinary technological advancements [13].

Bulk silicon is a poor light emitter of light owing to its indirect band gap semiconductor, in which radiative different from their bulk counterparts transition results in extremely weak light emission from silicon in the near infrared part of the spectrum [14]. Consequently there have been great efforts in last decade to produce controlled light emission from silicon in the near infrared and visible regions [15].

Nanostructure materials have generated intense research because the prossess physical characteristics which can be very different from their bulk counterparts. The main goal in the information technology is to have the possibility of integrating low – dimensional structures showing appropriate optoelectronic properties with well-established and highly advanced silicon microelectronics technology [16]. Silicon technology offers almost unlimited possibilities and pervades our everyday life. In addition it is possible to design these materials to a desired specification, these materials which containing nanometer sized particles have wide speared attention in recent years [17].

Among these nanomaterial is porous silicon (P-Si) which has high surface area morphology of hydride terminated silicon whose efficient room temperature luminescence has attracted much interest for a wide range of applications. The electrochemistry of semiconductors has played an important role in the development of integrated circuit (IC) technology.

Many of process used in IC manufacturing are based on electrochemical principles, and electro chemistry is the foundation for understanding the basic mechanisms of etching, deposition, and corrosion [6].

The light emitting properties were intriguing of several reasons; first: the emission energy was well above the band gap of bulk, second: the energy could be tuned throughout the visible spectrum by changing the preparation conditions an important consideration for display technologies that requires red, green and blue devices [1].

2.2. History of porous silicon

Porous silicon was discovered in 1956 by Uhlir [18] while performing electropolishing experiments on silicon wafers using an electrolyte containing hydrofluoric acid (HF). He found that under the appropriate conditions of applied current and solution composition, the silicon did not dissolve uniformly but instead fine holes were produced, which propagated primarily in the <100> direction in the wafer. Therefore, porous silicon formation was obtained by electrochemical dissolution of silicon wafers in aqueous or ethanoic HF solutions.

In the 1970s and 1980s the interest on porous silicon increased because the high surface area of porous silicon was found to be useful as a model of the crystalline silicon surface in spectroscopic studies, as a precursor to generate thick oxide layers on silicon, and as dielectric layer in capacitance based chemical sensors [8]

In the 1990s Leigh Canham [19] published his results on red- luminescence from porous silicon that was explained in terms of quantum confinement of carriers in nano-crystals of silicon which are present in the pore walls. Since that time, the interest of researchers and technologies to this material (and other porous semiconductors as well) is constantly growing and the number of publications dedicated to this class of materials increases every year.

When crystalline silicon (c-Si) wafers are electrochemically etched in hydrofluoric acid (HF) at specific current densities, pores are formed, which is known as a porous silicon (Psi) layer. This is an interesting material due to its unique and unusual optical and electrical properties compered to bulk silicon Si substrate. Structurally, Psi is very complicated [10]. On the other hand, Psi may

be considered as a system of interconnected quantum wells, the so-called quantum sponge. Nevertheless, the properties of Psi, such as porosity, thickness, pore diameter and microstructure of silicon, have been reported to depend on anodization conditions, including the electrolyte, current density, wafer type and resistivity, etching time and temperature [20].

The micro structural, chemical, electronic, and optical properties of porous silicon have been studied by various experimental techniques owing to large variety of Psi structures that can be produced by various techniques under different conditions. Among these techniques other methods were emerged, 1- electrochemical etching 2- laser annealing of amorphous silicon 3- anodization of bulk silicon 4- photoelectrochemical etching and 5- stain etching. The morphology and size of pores which produced by these techniques may be controlled by varying different conditions such as silicon doping, HF concentration, power density of the laser used and current densities etc… [21].

Much of the interest in Psi and its morphology derives from its PL properties which make it a useful platform for electronic and optoelectronic devices as well as chemical micro sensors. The first report of room temperature visible photoluminescence (PL) from porous silicon (Psi) structures has attracted wide interest in the scientific community]. Porous silicon can be fabricated from n-type and p-type crystalline silicon [22]. Structure and morphology of P-Si obtained by anodic etching of mono crystalline silicon in hydrofluoric acid HF depend highly on the doping level of silicon substrate and the degree of porosity.

To overcome this, several authors carried out stain etching of Si in HF/HNO3-based solutions and obtain porous layers similar to those prepared by conventional anodic etching [12].

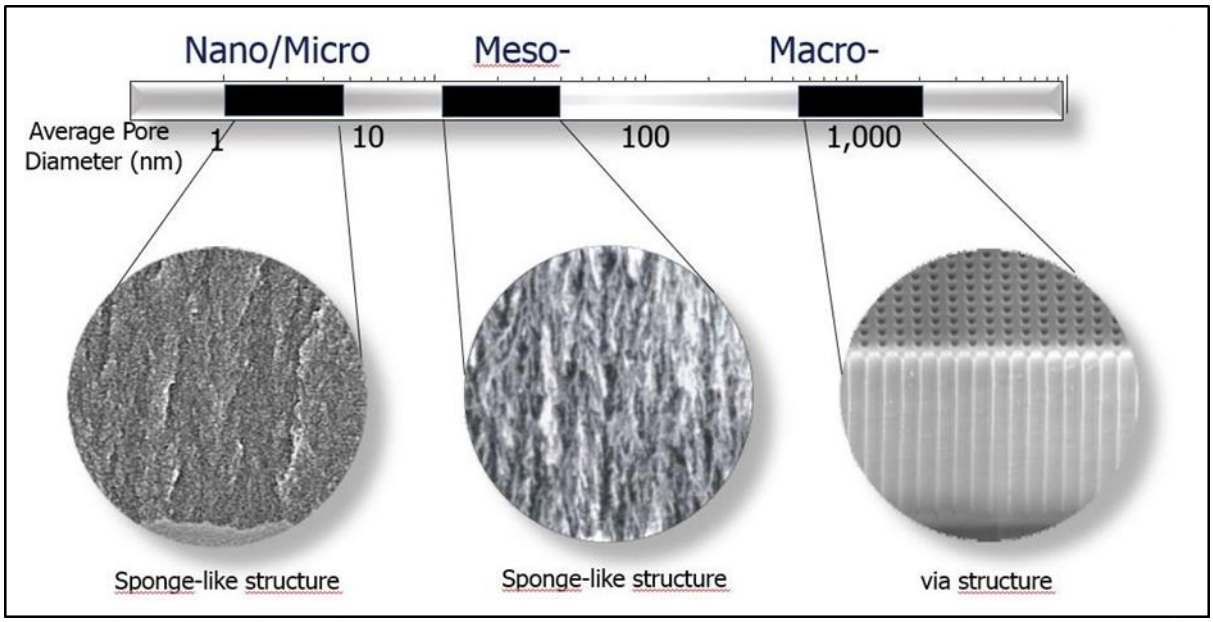

Figure (2-1):- the structures of porous silicon.

2.3. Crystalline Silicon

In the beginning of the nineteenth century the first semiconducting materials were studied. Since that time semiconductors have been the subject of extensive research. In the 1950s germanium was the most important material. However, germanium devices exhibited considerable leakage currents and additionally, germanium dioxide is a poor dielectric and chemically unstable. Silicon devices, on the other hand, exhibit much lower leakage and thermally grown silicon dioxide has excellent insulating and structural properties. This has made silicon the most widely used material in semiconductor device fabrication. Furthermore, the low cost compared to other semiconducting materials and the ease of processing has certainly contributed to the success of silicon in integrated circuit technology [23]

Silicon crystal has a diamond structure, with fcc braveries and lattice constant of 3.45 Ao and atomic number 14 as shown in figure (2-2).

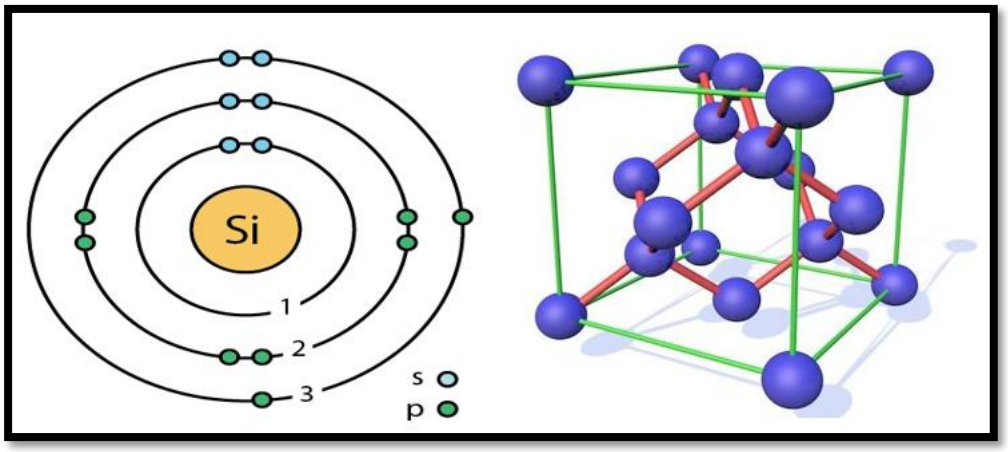

Fig (2-2): the lattice structure and atomic number of silicon.

In contrast to the good electrical characteristics of silicon, the light emitting properties are poor. Owing to the indirect band gap of 1.12ev, emission from bulk crystalline silicon is in the near – infrared and is very inefficient. For this reason the development of semiconductor optoelectronics has been dominated by the III – V compoundsemiconductors [24], many of which have a direct band gap as shown in figure (2-3).

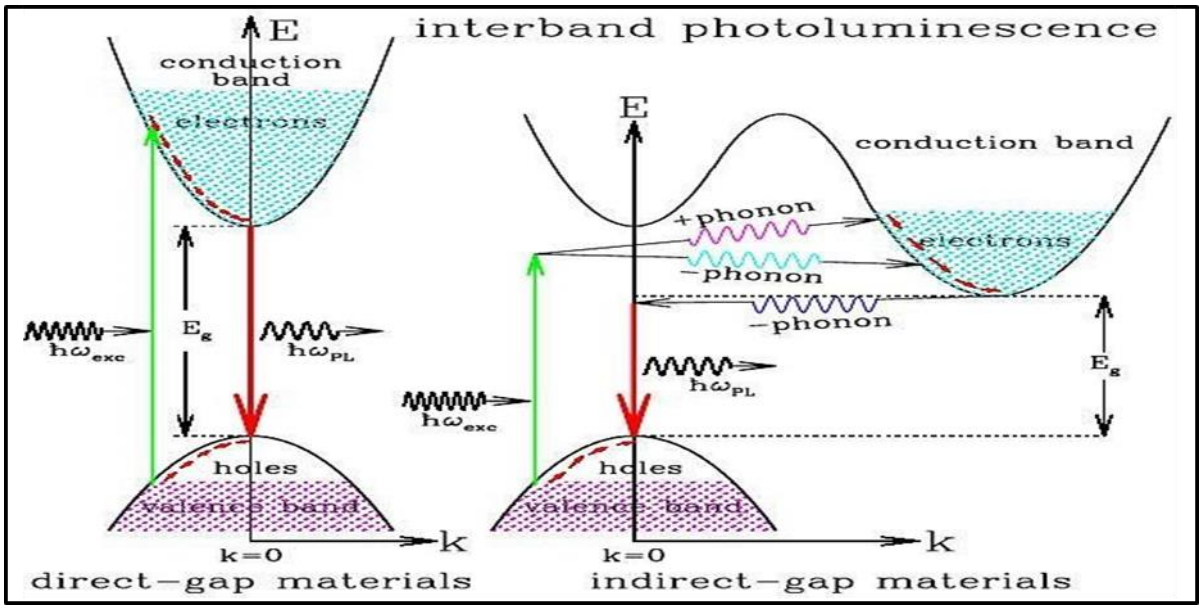

Fig (2-3): direct and indirect band gap of semiconductor

2.4. Quantum confinement

The study of dimensionality has a long history in chemistry and physics if we confined the excitons in a very small region, having dimensions of orders of a few nanometers we may also increase the radiative recombination rate and consequently the quantum efficiency. The small size of Si particles (ranging from 1 to 5 nm) in diameter exhibit PL emission ranging from blue to the near-infrared.

According to this model, P-Si emits light in the visible region at room temperature, owing to crystal in nanometer dimensions, which is different from bulk Si crystal whose band gap is in the far infrared region; the emission of P-Si at room temperature makes the QC model more valid than others[25]. Reducing dimensionality leads to major consequences in the electronic, optical, electrical and vibrational properties of the nanostructured material compared with the bulk. These

changes due to very significant characteristics such as:

1- zero dimensional confinement-:

In bulk semiconductor, the density of states D for electrons and holes using parabolic bands in the effective mass approximation. The function is sketched below showing the familiar square root dependence of the density of states in 3D reducing to zero as one approach the band edge.

2- One-dimensional confinement:-

So called quantum well, in this system, electrons are free to move in planes but their motions are confined in direction perpendicular to the planes. The situation is sketched schematically below showing a pair of 2D sub bands, at energy E0 and E1 respectively. The picture shows the confinement energy E0/1-Eg due to motional quantization a long Z-direction.

3- Two-dimensional confinement:-

So called quantum wire, the motion of electron occurs along one direction Away from the edge as shown below. The indices n,m of each one dimensional sub band denote the discrete kinetic energy quantum number for quantized motion along X or Y directions respectively.

4- Three- dimensional confinement:-

In quantum dot, the carriers are confined in all directions and kinetic quantization occurs along X, Y and Z directions and the energy spectrum is fully quantized. Figure (2-4) showing the density of states for the four above cases [26],

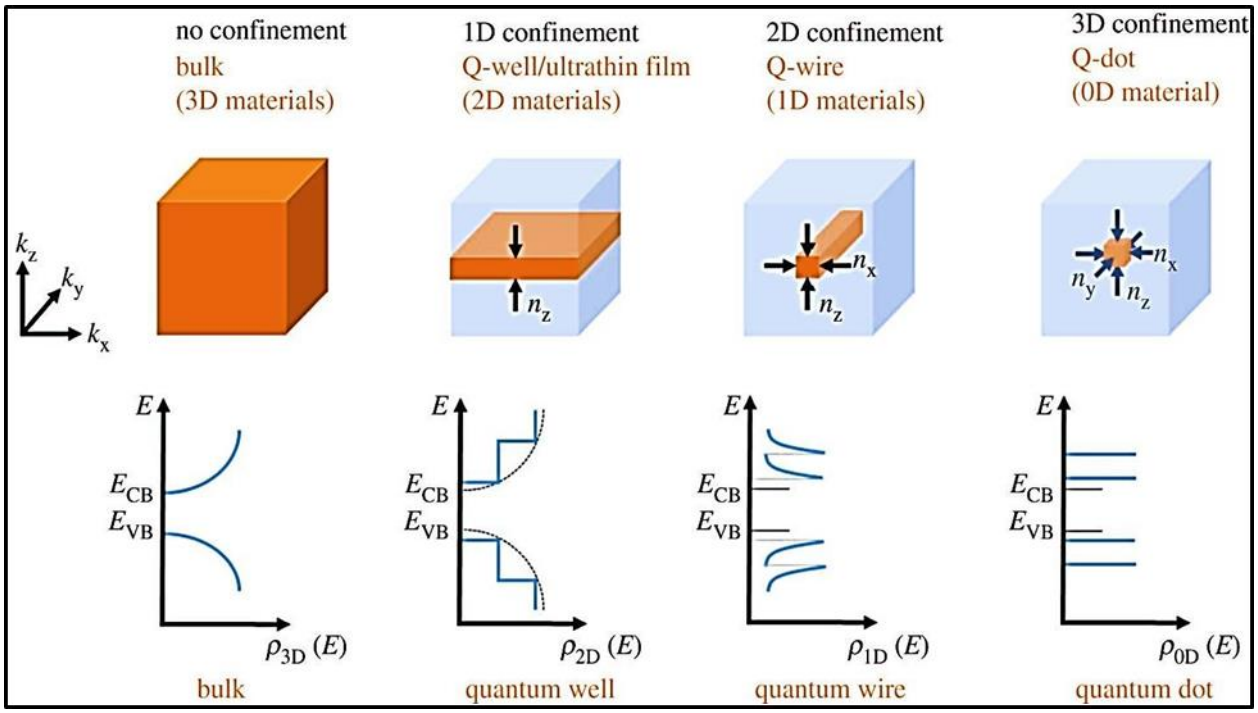

Fig (2-4): density of states for low dimensional structures.

2.5. porous silicon

Porous silicon has attracted a great deal of interest since Canham in 1990 reported observation of bright PL from P-Si even at room temperature. Psi is classified according to the pore diameter, which can vary from a few nanometers to a few microns depending on the formation parameters. The word nanoporous is sometimes used for smallest-pore regime to emphasize the nanometric dimension. An important parameter of a formed layer is porosity, which is defined as a ratio between the volumes of air voids to the total volume of P-Si layer [27]. The internal surface of P-Si per unit volume can be very large of the order 500 m2/cm3. The optical properties of porous silicon are drastically different from these of bulk crystalline silicon. Porous silicon shows an

increased band gap and efficient room temperature PL. Porous silicon is a special morphological form of silicon characterized by the presence of highly developed porous network in the silicon crystal [28].

2.5.1. Properties of porous silicon

Due to reducing the size in porous silicon all the properties of silicon will be deferent from the base material of silicon these properties include:-

A- Structural properties:-

Using these techniques the main properties studied are the morphology of the pore network and the crystalline dimensions. Structural properties of P-Si have been investigated by scanning electron microscopy (SEM) which the direct imaging of the material could be carried out, although the resolution achievable (down to < 2 nm) and the available contrast make it difficult to visualize the smallest structures, X-ray scattering in these techniques small angle scattering measurements allow the determination of nanostructure dimensions and alignments, the surface area per unit volume and the sharpness of the Si interface with internal voids, and X-ray absorption can give information on the band gap and local atomic order of the material [16].

Atomic force microscope (AFM) gives a direct surface image but with restricted lateral resolution, and Raman spectroscopy gives the size of nanocrystallited dependent on vibrational frequencies [29].

B-Vibrational properties:-

The confinement of vibrations in nanocrystals leads to shift in the Raman line Frequency as well as a change in the Raman line shape involving both is broadening an asymmetry. These changes are functions of the nanocrystallite sizes. Different models have been used to study confinement effects on the vibrational properties such as the phonon confinement model [30].

C-Optical properties -:

Optical properties of semiconductor nanocrystals largely dependent on surface properties as well as on the surrounding matrix [4]. The optical properties such as nonlinearity associated with changes in refractive index are significantly affected by presence of nanocrystallites and size distribution of nanocrystallites. This can lead to well-known phenomena of self – focusing and self – phase modulation [2]. For any application of a material in optics or optoelectronics it is essential to know its refractive index. A very simple method to evaluate the refractive index for a film – like material is to measure the interference fringes, due to multiple reflections, in order to obtain the optical thickness [31].

D-Electrical properties:

Electrical resistivity in Psi is five orders of magnitude higher than in intrinsic Si, because Psi is depleted by free carriers. Depletion can occur either because of the energy gap widening from quantum confinement which reduces the thermal generation of free carries, or because trapping of free carriers [1]. Trapping can occur during the preparation of Psi either because the binding energy of dopant impurities is increased or because the formation of surface states.

2.5.2. Preparation method of porous silicon

1- Electrochemical etching-:

The electrochemical etching process is performed hydrogen fluoride solution (HF). As to etching rates, they are controlled by adjusting the electrolyte compositions and etching current densities it is well-known that the etching current is governed by the hole concentration in the adjacent regions of HF electrolyte and Si atoms to assist anodic oxidation during the electrochemical etching.

The anodization can be formed either in potentiostatic (voltage –controlled) or in galvanostatic (current – controlled) made, the later is normally preferred, because it supplies the required charge

of the reaction at constant rate, regardless of any evolution during anodization of the cell electrical impedance, ultimately leading to more homogeneous and reproducible material [32]. Figure (2-5) show steps of electrochemical etching process

2-Photochemical etching:-

In laser – induced etching process a Si wafer is immersed in aqueous HF acid and irradiated with laser radiation of appropriate wave length and power density, electron – hole pairs are generated in the irradiated area and a depletion layer is formed. A chemical reaction takes place involving the photo generated holes and the fluorine ions.

Pore formation take place as a result of silicon atoms detachment from the wafer in the form of SiF3 and SiF4 [2]. During laser induced etching, n – type crystalline – silicon (C-Si) substrate is irradiated with laser light in HF acid there by creating excess holes on the irradiated surface. Subsequently, a depletion layer is formed in the silicon substrate and it results in a net electron flow through the electrolyte solution to the irradiated surface [33].

3-chemical etching:-

The stain etching is another technique, which can be used to produce films similar in nature to the anodically prepared P-Si. This method is an intrinsically easier and less frequently employed technique which is used an open – circuit consisting essentially of HF: HNO3:H2O.

Etching the silicon in this method reduced the size and passivated the surface of these materials such that after etching they exhibited bright visible PL at room temperature [20]. The etching process will be initiated after a time interval of approximately 1 or 2 minutes, called the incubation time. It is found that the incubation time for p-type samples increases with increasing sample resistivity but for n-type samples, the incubation time is weakly affected by the sample resistivity and this time was found to be longer than that for p-type samples and it is in the range of 8-10 minutes. The stain etching reaction of silicon can be written as [21]:-

$Si + HNO3 + 6HF \rightarrow H2SiF6 + HNO2 + H2O + H2.$

4- Photoelectrochemical etching:-

PEC etching has been used to fabricate unique structures in electronic and photonic devices especially of III – V semiconductors; because of the need for optical components in III – V based light wave systems and the ease of PEC process due to the solubility of reaction product.

The semiconductor is immersed in a conductive electrolyte, and electrical contact is made to the semiconductor is biased with respect to a counter electron. When the Fermi level of semiconductor at the semiconductor – electrolyte interface in with in the band gap, the density of carriers in the semiconductor is usually less than the density of carriers in the electrolyte, so that a majority of the potential difference across the interface occurs with in the semiconductor Figure (2-6) shows the case of on n-type and p-type in the contact with an electrolyte [34].

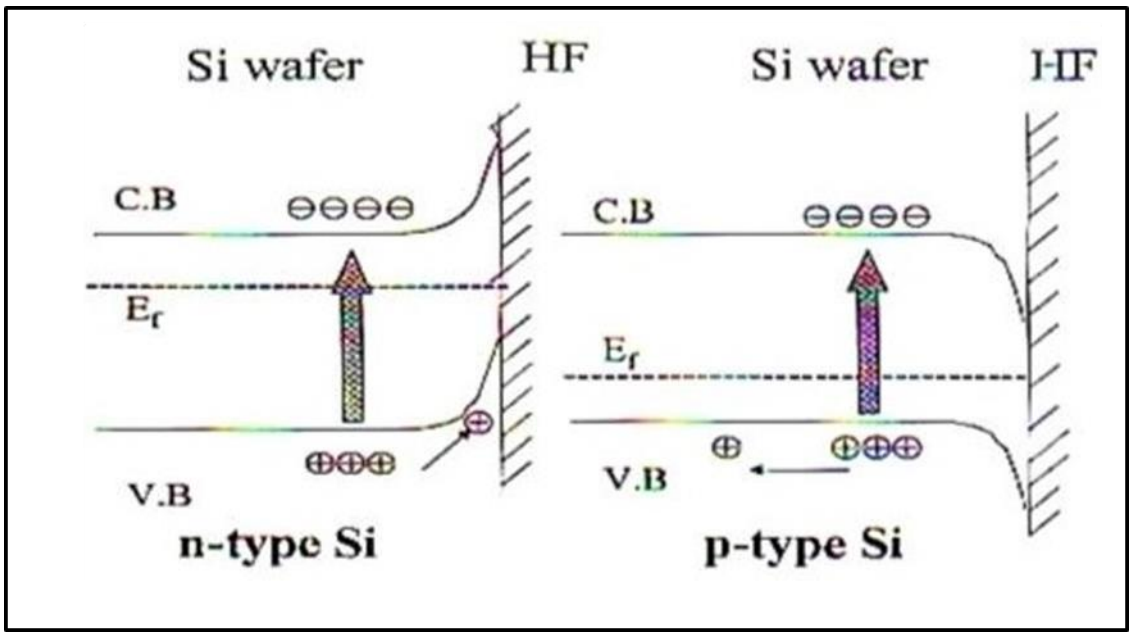

Fig (2-6): energy structure of an (n and p type (semiconductor in contact with an electrolyte.

2.6. Porous silicon formation is influenced by the following parameters:-

- ✓ The substrate doping.
- ✓ The current density (which determines the depletion width and the Carrier injection rate).
- ✓ The HF concentration.
- ✓ The solvent where the HF is diluted.
- ✓ The etching time: longer etching time lead to thicker layers, but for Long times an anisotropy in depth in the layer due to chemical action of the electrolyte is introduced.
- ✓ The illumination during the etch

1.7. SERS Substrates:-

The conditions of success for the SERS studies are highly rely on the plasmonic nanostructure surface interaction with the absorbed probe molecule. A big efforts have been exerted for research on metal nanoparticles synthesis that because of the possible applications for novel technologies development. Silver (Ag), gold (Au), palladium (Pd) and copper (Cu) nanoparticles metals represent the most utilized substrates in SERS that are a powerful candidates owing to their stability and biocompatibility. Most Raman measurements have been occurred in the wavelength range from visible to near infrared figure (2-7), all the metals have been mentioned above carry on LSPR [35].

Moreover, experiments of SERS have been carried out with another nanoparticles of metals such as ruthenium (Ru), rhodium (Rh), aluminum (Al) and platinum (Pt). Semiconductors as quantum dots (QDs) and TiO2.

Novel materials like graphene, have been recently reports to exhibit SERS, although they do not fit traditional SERS definitions substrates [36].

When a material has been classified as a dependently and highly enhancing SERS substrate, many factors must be taken into account. In any way, SERS-active substrates could be classified into three categories as following:

Metallic electrodes, planar metallic structures, metallic nano-particles like arrays supported over planar as (Si, metals and glass, etc) substrates. Finally, nanoparticles of metallic in suspension, as

colloidal solutions [37].

One of the easiest and simplest route to SERS represented by metal colloids in suspension or immobilized, that usually made of Ag or Au, because the colloidal synthesis is relatively easy. Many process have been developed in this field to synthesis colloidal nanostructures for activity of SERS that remain to nowadays [24].

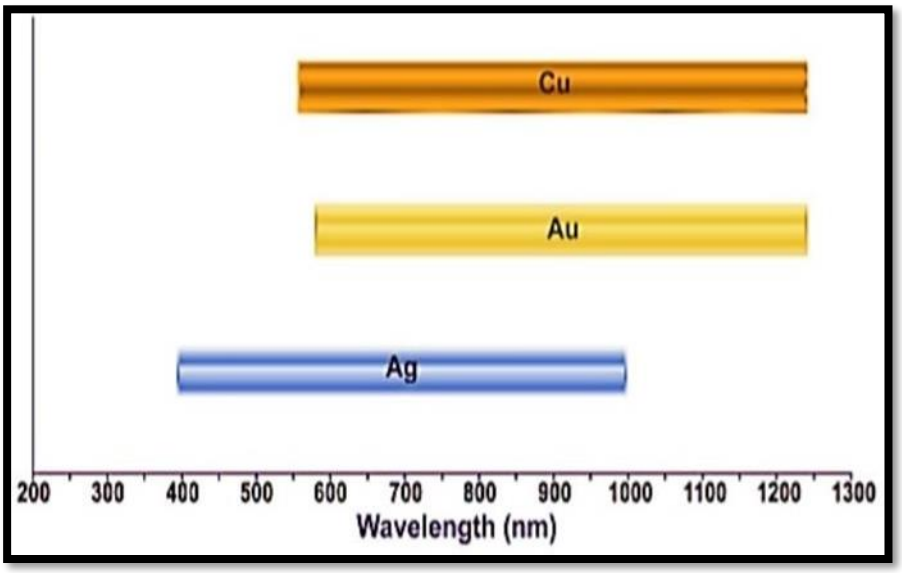

Fig (2-7): Wavelength ranges for Ag, Au, and Cu that support SERS

1.8. Applications of porous silicon

A variety of applications for porous silicon have emerged since it was first discovered. It has already been noted that possible applications for porous silicon have been found in dielectric isolation of integrated circuits and various optoelectronic applications table (2-1) show most of porous silicon applications [25].

Application area	Role of porous silicon	Key property
Optoelectronics	LED	Efficient electroluminescence
	Waveguide	Tunability of refractive index
	Field emitter	Hot carrier emission
	Optical memory	Non-linear properties
Micro-optics	Fabry-Pérot Filters	Refractive index modulation
	Photonic bandgap structures	Regular macropore array
	All optical switching	Highly non-linear properties
Energy conversion	Antireflection coatings	Low refractive index
	Photo-electrochemical cells	Photocorrosion cells
Environmental monitoring	Gas sensing	Ambient sensitive properties
Microelectronics	Micro-capacitor	High specific surface area
	Insulator layer	High resistance
	Low-k material	Electrical properties
Wafer technology	Buffer layer in heteroepitaxy	Variable lattice parameter
	SOI wafers	High etching selectivity
Micromachining	Thick sacrificial layer	Highly controllable etching
Biotechnology	Tissue bonding	Tunable chemical reactivity
	Biosensor	Enzyme immobilization

3-2. experimental instruments

The following instruments have been used in this work.

3-2-1. laser source

We have used the commercially available CW diode laser source of constant power have been employed in chemical process assisted with laser. We used CW diode laser of a wavelength (532 nm) with an output power of 5mW was also used as an illumination source for reconstruction the surface during the stain etching to produce multilayer PSi.

3-2-2. Chemical Materials

Hydrofluoric acid 40%, (HIMEDIA), Gold (III) chloride trihydrate (HAuCl4. 3H2O) with 99% purity, supplied from (CDH), India was used as received, high purity ethanol 99.99% were purchased from Sigma Aldrich. 40 M HF was diluted with ethanol to obtain the etching HF solution at 20 M concentration.

Scanning electron microscope and optical microscope

The surface morphology carried out by using scanning electron microscopy SEM (TEScan – Vega II SBH) and we have used the optical microscope of (600X) maximum magnification power types to studies the topography of the porous silicon surface which prepared under different conditions. The microscope has a digital camera to capture image by a personal computer. The etching rate was determined by measuring the maximum PSi layer thickness at the spot center. The etching rate could be calculated by the simple relation [25].

Maximum etching rate = maximum thickness of PSi (μm) / irradiation time (min). (2-1)

3-3. silicon sample preparation

Silicon samples which used in this work were p-type Si of orientation (111) with a resistivity of 1.5-4 Ω.cm and cut into a size of 1*1 cm2 pieces prepared and cleaned with a sequence of chemicals which do not attack the Si material but selectively remove any contamination on the surface.

3-4. experimental set-up

A simple set-up in our experiment has been used for stain etching process. The set-up consists of a CW laser source, focusing lens and the etching acids in a plastic container. The samples used in this project were n- type Si (111). They were degreased using organic solvents, followed by oxide removal with 40% HF solution, finally rinsed in de-ionized water. The laser source was vertically mounted by a holder above the sample, aligned and focused by quartz lens of a focal length 5 cm to achieve a circular spot. Porous silicon was prepared by chemical etching using an electrolyte containing 40% HF (1:3) acids at room temperature for time within 10 to 20 min with illuminating 5mW laser diode light λ=532 nm onto the sample surface. After stain etching the samples were rinsed in de-ionized water. The surface morphology of stained sample was examined by using scanning electron microscopy. The experimental set-up illustrated in figure (3-1).

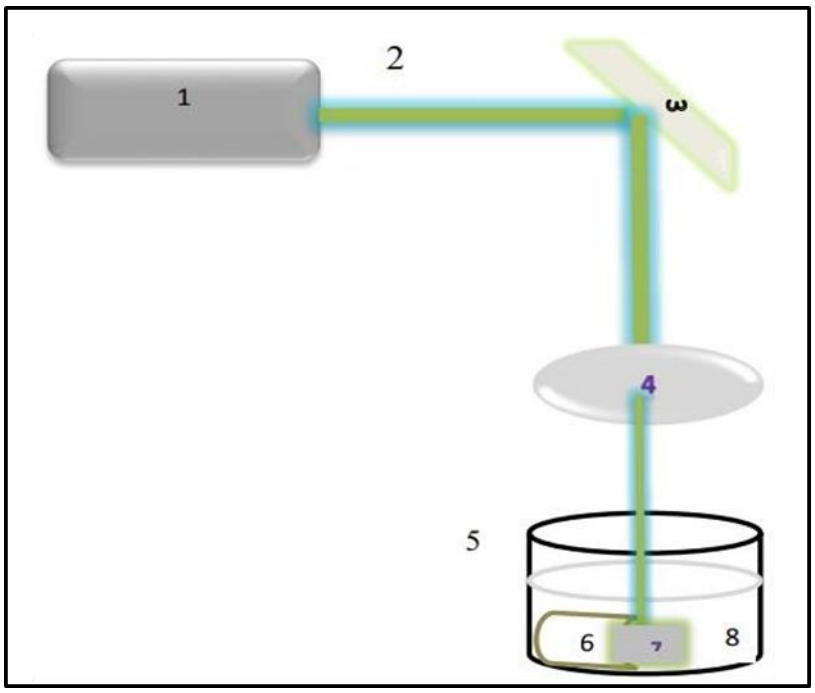

Fig (3-1):- Schematic diagram of chemical etching assisted with laser set up:

(1) diode laser; (2) laser beam; (3) reflecting mirror; (4) focusing lens; (5) container;

(6) Teflon; (7) silicon sample; (8) HF acid.

1-1 Morphological Features of the PS Samples

The surface topography which depend on the etching conditions are the most important morphological parameters of PS layer. These parameters and the parameters of the immersion plating effect on the size and arrangement of AuNPs. Hence, to form SERS – chemical sensor, the morphology of PSi samples and the immersion plating parameters must be tuned.

1-1-1 Surface Morphology of the Bare PS samples

Figure (4-1 a&b) show the surface morphology of PS layer which was prepared at four etching times of (5 to 20) min, respectively. The structure of PSi samples is a pore look like, and is spherical, and the pores are randomly distributed on the surface. From figures we found the etching time with 20 min have higher depth with regular pores like structure from the other etching time.

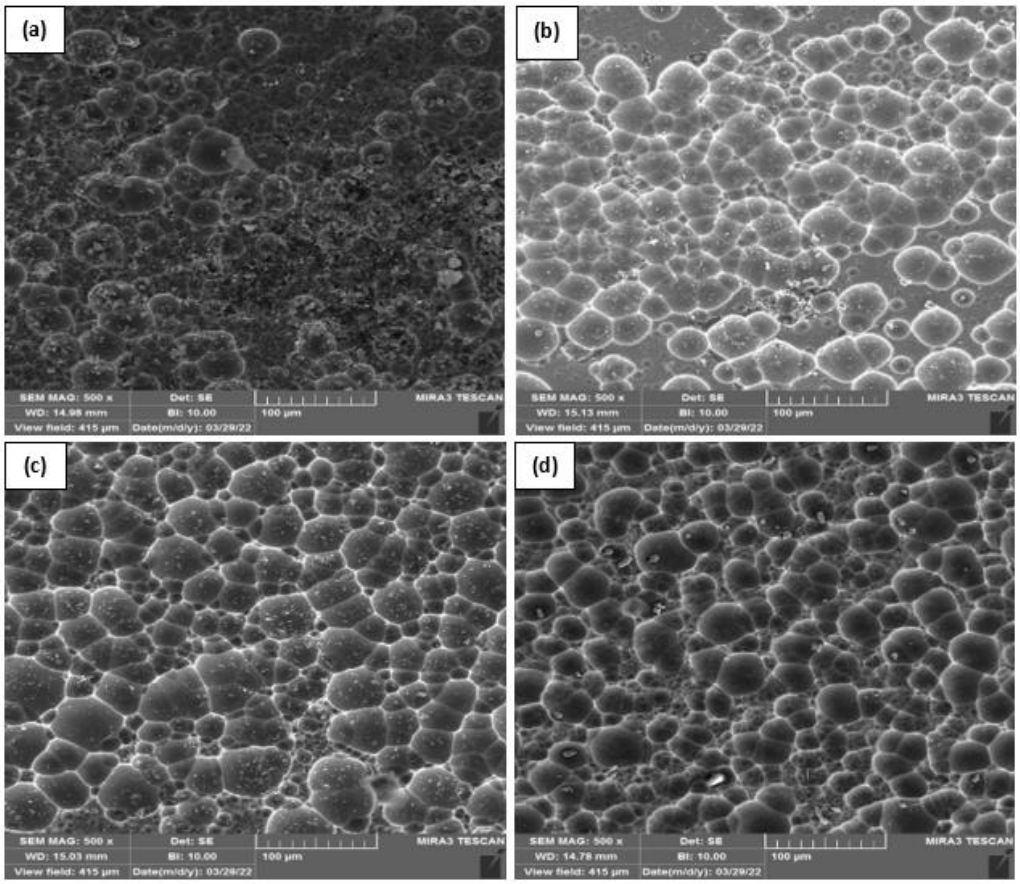

Fig.(4-1) SEM images of PS surface with etching time of (a) 5 min, (b) 10 min, (c) 15 min and (d) 20 min.

1-2 Porosity, Thickness and Etching Rate

The main structural parameters of the porous silicon are porosity and porous thickness. The influence of the formation time on etching rate and porous silicon layer thickness were cleared in figure (4-2a and b) respectivly. The porosity of samples were estimated by using the equation(21):-

$$P(\%) = \frac{m1 - m2}{m1 - m3} * 100$$

Where (m1) the weight of samples before anodization, (m2) the weight of samples after anodization and (m3) the weight of samples after dissolution porous silicon in NaoH solution.

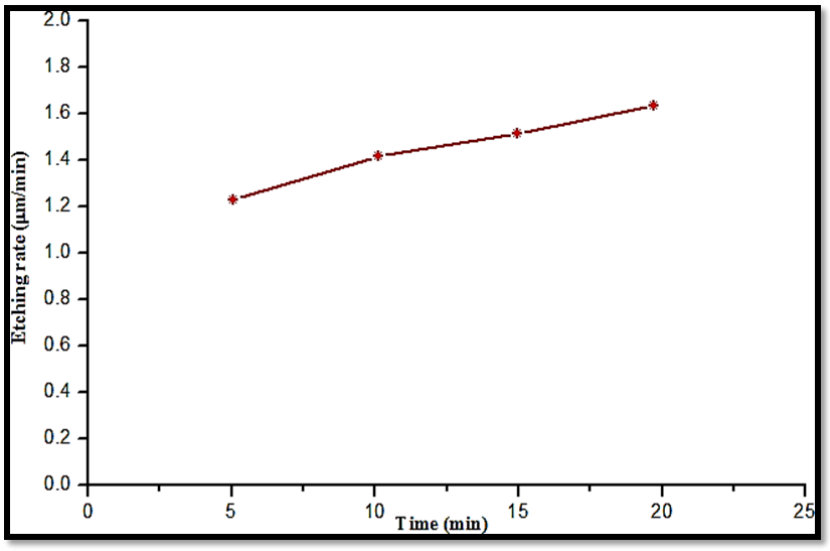

A linear increase in the thickness enhancement from 6.27 to 30.60 μm with an increasing etching time can be observed. This lead to increasing in the etching rate which depend on the porous layer thickness and these suggests that etching times led to increasing in pore growth and the underlying reason was thought to be attacking directly of F– ions on Si atoms. However, when the formation time increased, another process of decay, i.e., chemical dissolution began to prevalent. These methods were common at the wall of pores and suppressed the intraction at the pore tip. Consequently, inter-pore distance becomes narrower with an increasing formation time. The surface porosity of PSi layer expantion with formation time which illustrated in figure (4-2c). It is approbate that the porosity variation with layer thickness were owing to the chemical dissolution of porous silicon material through etching process. Through the reaction of the electrochemical process, and as a function of the formation time, theinflunce of chemical dissolution were to increase the pores diameter also the average of porosity.

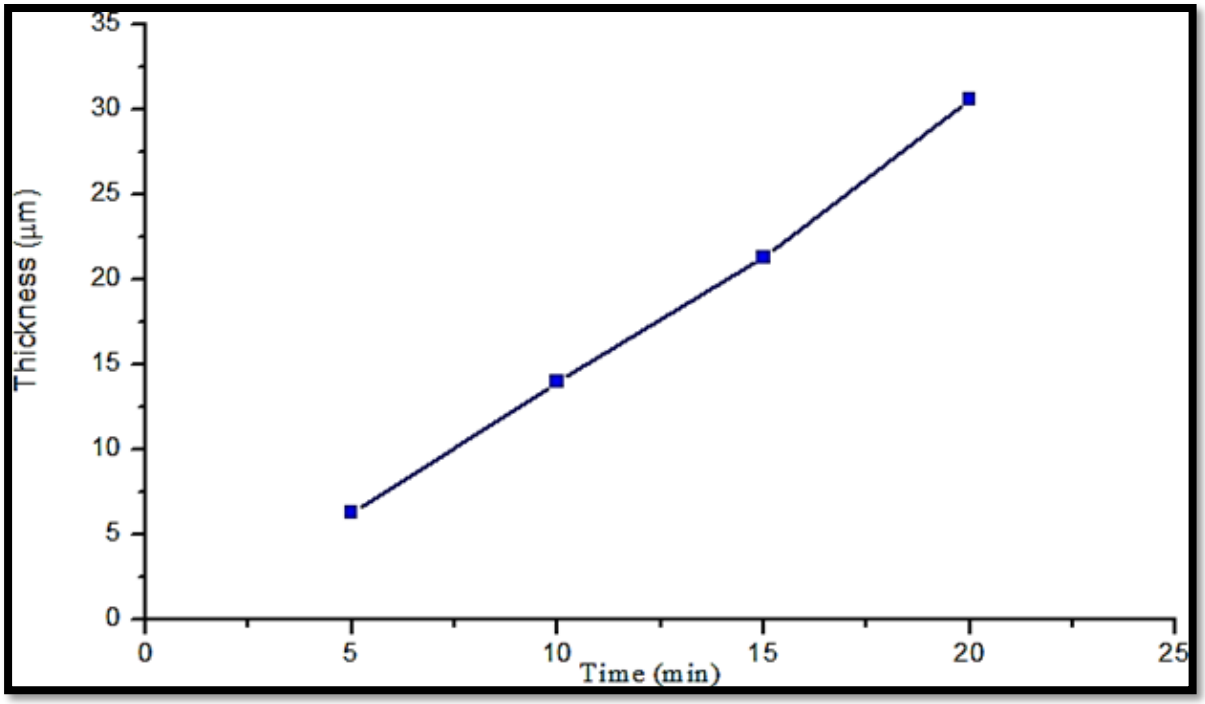

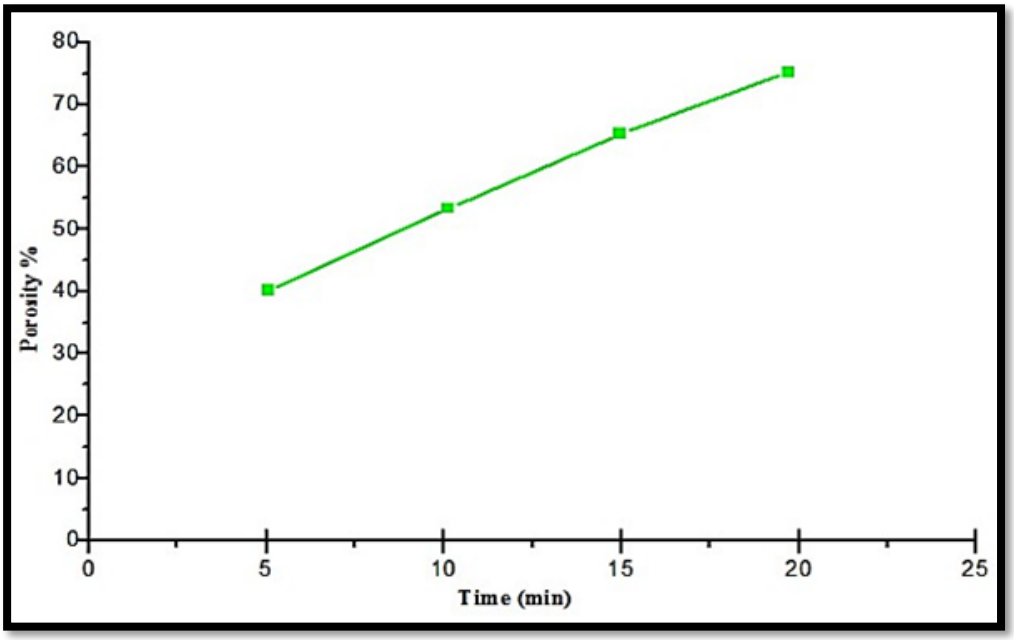

Fig (4-2): the relation between etching time with a) thickness b) porosity c) porosity for etched samples.

1-3 Surface Morphology of the AuNPs/ PSi Sensors

For the sample have been prepared with optimum conditions of 20 min etching time laser effects of metallic deposition AuNPs on PSi substrates have been illustrated in figures (4-3). This figure shows the 3-D micro images and morphology of AuNPs that deposited on PSi layer. It illustrates the AuNPs profiles show a large accumulation of particles that change the surface roughness and so the depth of surface. Size, densities as well as arrangement of the AuNPs rely on morphology of the essential PSi based layer. These surface topographical properties variations are due to high density nucleation sites and high density metallic ions; resulted from the reduction process.

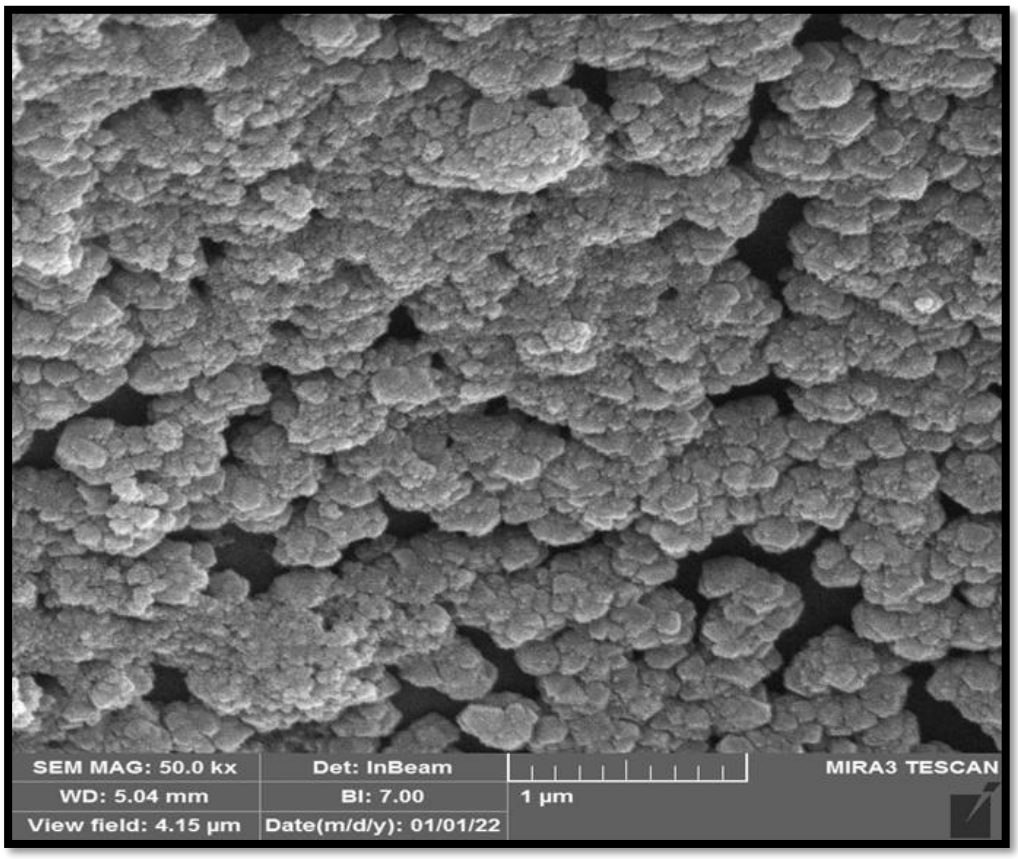

Sensing Performance of Metallic as SERS Chlorpyrifos Pesticides Sensors.

The sensing properties of PSi substrates which prepared with optimum condition of 20 min etching time was tested after deposition of gold and silver nanoparticles. The AuNPs/PSi SERS pesticides sensors have been tested with chlorpyrifos pesticide. The Raman and SERS spectra features of the chlorpyrifos pesticide sensors are illustrated in figure (4-4). For bare PS layer without any metallic nanoparticles, the sensor performance for chlorpyrifos solution showed very weak Raman response; even at high (10-2 M) chlorpyrifos concentration. The intensity of Raman peak increased dramatically after incorporating the Au nanoparticles on PSi. This has resulted from the plasmonics effects of metals nanoparticles (hotspot junctions and nanoparticles sizes). The fabricated PSi with Au nanoparticles SERS pesticides sensors were tested under different chlorpyrifos concentrations: 25□10-8 , 12□10-7 , 6□10-6 and 3□10-5 M.

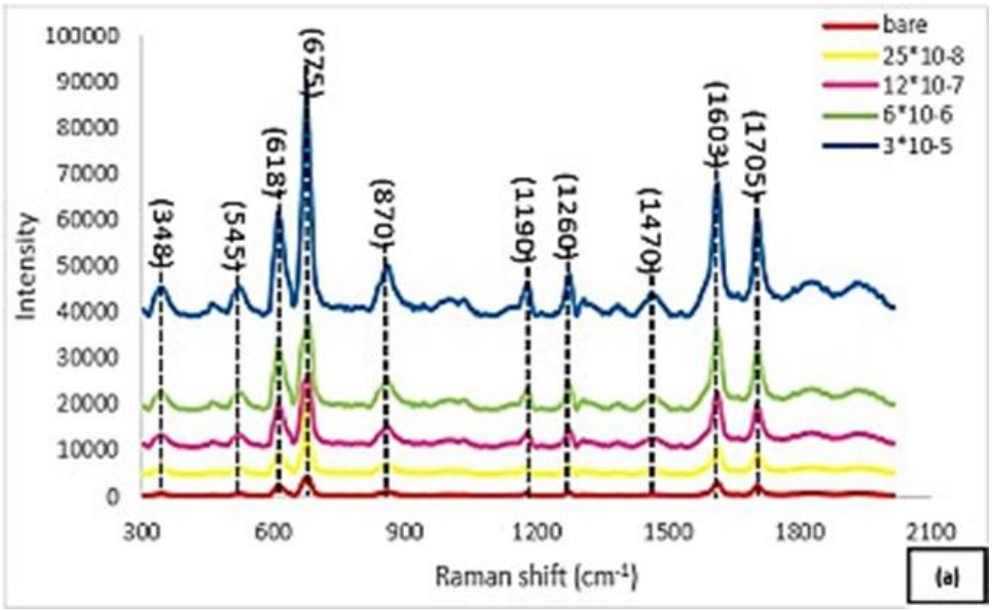

Fig. (4-4) Raman spectra of (a) AuNPs/PSi prepared with 20 min for chlorpyrifos pesticides

Conclusions

We have been formed and characterized the layer of porous silicon to study its morphological, structural characteristics. Influence of formation time on the structural and morphological properties have been investegated by using SEM. SEM show that porous silicon layer has a uniform structure and this structure varied with increasing the etching time. The optical microscope were carried out to study the thickness, and etching rate of porous silicon layer we have found the porous silicon thickness increases from 6.27 to

30.60 µm with increasing the etching time. The etching rate was found to be increase from 1.25 to 1.53 µm/min also the porosity of porous layer. The scanning electron microscope revealed many irregularly shaped pores and cracks distributed randomly over the entire surface. Such a surface topography is the same as those commonly observed on the conventionally stained surfaces. However, the microscopically roughened layers were formed on all etched surfaces. SERS sensors could be produced by immersion process of porous silicon structures in metallic ions solutions. The metal deposited as well as substrate features represent the keys of sensor operation for efficient detection.

References

1. Megha M., Uday V. and Ashwin V. “Classification of pesticides: A Review” Int. J. Res. Ayurveda Pharm. 9 (4), 2018: 144-150.
2. Shintaro P., Tianxi Y. and Lili H. “Review of Surface Enhanced Raman Spectroscopic (SERS) Detection of Synthetic Chemical Pesticides” TrAC Trends in Analytical Chemistry, 85 Part A, 2016: 73-82.
3. Fernando P. “Pesticides, environment, and food safety” Food and Energy Security 6(2), 2017: 48–60.
4. Hermann B. “Immunoassay of Pesticides” In: Gilbert L.I., Miller T.A. (eds) Immunological Techniques in Insect Biology. Springer Series in Experimental Entomology. Springer, New York, NY, 1988: 135-179.
5. Roy Z., Ricardo S., Oscar R. and Seiling V. “What are the Main Sensor Methods for Quantifying Pesticides in Agricultural Activities? A Review” Molecules, 24(14), 2019: 2659.
6. Mehmet K., Emma R., Aysun K. and Sebastian W. “Fundamentals and applications of SERS-based bioanalytical sensing” Nanophotonics 6(5), 2017: 831–852.

7. Mingming H., Hongmei L. and Zhimin Z. “Fast and Low-Cost Surface-Enhanced Raman Scattering (SERS) Method for On-Site Detection of Flumetsulam in Wheat” Molecules 25, 2020: 4662.
8. Allaa A. Jabbar, Alwan M. Alwan and Adawiya J. Haider “Modifying and Fine Controlling of Silver Nanoparticle Nucleation Sites and SERS Performance by Double Silicon Etching Process” Plasmonics 13, 2018: 1171–1182.
9. Zhai C., Li Y., Peng Y. and Xu T. “Detection of chlorpyrifos in apples using gold nanoparticles based on surface enhanced Raman spectroscopy” Int J Agric & Biol Eng. 8(5), 2015: 113-120.
10. Xuexian C., Jinxiu W., Jianhua Z., Zebo Z., Di A., Hao W., Weiguang X., Runze Z., Ningsheng X., Jun C., Juncong S., Huanjun C. and Shaozhi D. “Superhydrophobic SERS substrates based on silicon hierarchical nanostructures” J. Opt. 20,2018: 024012.
11. Yong H., Shupei X., Tao D. and Pengcheng N. “Gold Nanoparticles with Different Particle Sizes for the Quantitative Determination of Chlorpyrifos Residues in Soil by SERS” Int. J. Mol. Sci. 20, 2019: 2817.
12. Bingxue H, Da-Wen S., Hongbin P. and Qingyi W. "Rapid nondestructive detection of mixed pesticides residues on fruit surface using SERS combined with self-modeling mixture analysis method" Talanta, 217, 2020:120998.
13. Ossicini S., Pavesi L., and Priolo F. “Light emitting silicon for microphotonics” Springer Science & Business Media 194, 2003.
14. Marya A. “Chapter 16 - Nanomaterial synthesis” Editor(s): Ravin Narain, Polymer Science and Nanotechnology, Elsevier, 2020: 361-399.
15. Ibrahim K., Khalid S. and Idrees K. “Nanoparticles: Properties, applications and toxicities” Arabian Journal of Chemistry 12(7), 2019: 908-931.
16. Ronja K., Nils W., Jörg K. N. and Cedrik M. “High-precision determination of silicon nanocrystals: optical spectroscopy versus electron microscopy” Semicond. Sci. Technol. 34, 2019: 095009.
17. Hee H., Zhipeng H. and Woo L. “Metal-assisted chemical etching of silicon and nanotechnology applications” Nano Today, 9(3), 2014: 271-304.
18. Uhlir A., " Electrolytic shaping of germanium and silicon " bell system Tech. 35 (1956) 333.
19. Canham, L. T., "Silicon quantum wire array fabrication by electrochemical and chemical dissolution of wafers", Appl. Phys. Lett., 57 (1990) 1046.
20. Xiaoyu C. and Bin G. “Optical Biosensing and Bioimaging with Porous Silicon and Silicon Quantum Dots” Progress In Electromagnetics Research 160, 2017: 103-121.
21. Hadeel F. S. and Bassam G. R. “Self-Phase Modulation of Silicon Nanostructure Produced By Laser Induced Etching” NUCEJ, 91(1), 2016: 137 – 144.
22. Xiao-Cheng D., Shuo H., Ming-Hui H., Yu-Bing L., Tao L. and Fang-Xing X. “Electrochemically anodized one-dimensional semiconductors: a fruitful platform for solar energy conversion” J. Phys. Energy, 1, 2019: 022002.
23. Olga V., Sergey G. and Petr L. “Influence of Illumination on Porous Silicon Formed by Photo-Assisted Etching of p-Type Si with a Different Doping Level” Micromachines, 11(199) 2020.
24. Bhandari R., Negi S., Rieth L and Solzbacher F. “A Wafer-Scale Etching Technique for High Aspect Ratio Implantable MEMS Structures” Sens Actuators A Phys., 162(1), 2010: 130-136.
25. Kahtan K., Bassam G. R., Mohemmed A. I. and Arina F. M. “Effect of laser-induced etching process on Porous structures” Procedia Engineering 38, 2012: 1381 – 1390.

26. Alwan M.A., Adawyia J. H., and Allaa A. J., “Study on Morphological and Structural Properties of Silver Plating on Laser Etched Silicon” Surface & Coatings Tech. 283, (2015), 22-28.

27. Zaichun L., Xinhai Y., Shuaishuai Z., Jing W., Qinghong H., Nengfei Y., Yusong Z., Lijun F., Faxing W., Yuhui C. and Yuping W. “Three-dimensional ordered porous electrode materials for electrochemical energy storage” NPG Asia Mater., 11(12), 2019.

28. Emily J. A., Lingyun C., William R. F. and Michael J. S. “Porous silicon in drug delivery devices and materials” Advanced Drug Delivery Reviews 60(11), 2008: 1266- 1277.

29. Jayanta K. P., Gitishree D., Leonardo F. F., Estefania V. R., Maria d. P. , Laura S. A., Luis A. D., Renato G., Mallappa K. S., Shivesh S., Solomon H. and Han-Seung S. “Nano based drug delivery systems: recent developments and future prospects.” Journal of nanobiotechnology, 16(1) 71. 2018.

30. Claudia P. “Photonic Crystal Sensors Based on Porous Silicon” Sensors, 13 2013: 4694-4713.

31. Ferrando-Villalba P., D’Ortenzi L., Dalkiranis G. G., Cara E., Lopeandia A. F., Abad Ll., Rurali R., CartoixàX., De Leo N., Saghi Z., Jacob M., Gambacorti N., Boarino L. and Rodríguez-Viejo J. “Impact of pore anisotropy on the thermal conductivity of porous Si nanowires” Sci Rep, 8, 2018: 12796.

32. Kuen-Hsien W. and Chong-Wei L. “Light Absorption Enhancement of Silicon- Based Photovoltaic Devices with Multiple Bandgap Structures of Porous Silicon” Materials, 8, 2015: 5922-5932.

33. Shereen M. F., Shaimaa A., Nasreen R. and Johnny F. “Porous Silicon Morphology: Photo-Electrochemically Etched by Different Laser Wavelengths” Journal of Nanotechnology in Engineering and Medicine, 6(1), 2015.

34. Tuang Y. P., Nur B., Micheál M. A., Mustafa H. K., Magdiel I. S., Kee W. N. and Sanjay H. C. “Inhaled nanomaterials and the respiratory microbiome: clinical, immunological and toxicological perspectives” Particle and Fibre Toxicology, 15(46), 2018.

35. Liangliang Y., Jiangtao W., Zhe M., Peishuai S., Jing M., Yongqiang Z., Zhen H., Mingliang Z., Fuhua Y. and Xiaodong W. “The Fabrication of Micro/Nano Structures by Laser Machining” Nanomaterials (Basel, Switzerland), 9(12), 2019: 1789.

36. Kurt K. “Silicon nanostructures from electroless electrochemical etching” Current Opinion in Solid State and Materials Science 9(1-2), 2013: 73-83.

37. Maurizio C., Giuseppe C., Mario I., Ivo R. and Luigi S. “Near-Infrared Sub- Bandgap All-Silicon Photodetectors: State of the Art and Perspectives” Sensorsm 10, 2010: 10571-10600.